Available online at www.sciencedirect.com
ScienceDirect
Physics Letters A 359 (2006) 161–165
PHYSICS LETTERS A
www.elsevier.com/locate/pla

Hydrogenic impurity states in a wurtzite InGaN quantum dot

C.X. Xia *, S.Y. Wei

Department of Physics, Henan Normal University, Xinxiang 453007, People's Republic of China

Received 17 April 2006; received in revised form 12 May 2006; accepted 8 June 2006

Available online 21 June 2006

Communicated by J. Flouquet

Abstract

Within the framework of effective-mass approximation, we calculated variationally the binding energy of a hydrogenic donor impurity in a cylindrical wurtzite (WZ) InGaN/GaN strained quantum dot (QD), including the strong built-in electric field effect due to the spontaneous and piezoelectric polarizations. It is found that the donor binding energy is highly dependent on the impurity position and QD size. In particular, we found that the donor binding energy is independent of dot height when the impurity is located at the right boundary of the WZ InGaN strained QD with large dot height ($\geqslant 2.5$ nm).
© 2006 Elsevier B.V. All rights reserved.

PACS: 73.21.La; 71.55.-i; 77.65.Ly

Keywords: Quantum dot; Hydrogenic impurity; Built-in electric field

1. Introduction

In recent years, the wide-band-gap group-III nitrides based semiconductor heterostructures InGaN/GaN have attracted much attention due to conspicuous device applications in electronics and optoelectronics, such as high-brightness blue/green light-emitting diodes (LEDs) and laser diodes (LDs) [1,2]. It has been found that many nanometer-scale In-rich islands called In-rich quantum dots (QDs) are spontaneously formed within the InGaN active layer in wurtzite (WZ) InGaN/GaN quantum heterostructures [3–6]. In such nanometer-scale In-rich QDs, the charge carriers are confined in all three dimensions (3D) [7]. On the other hand, the group-III nitrides are commonly produced in the WZ crystal structure with a strong spontaneous macroscopic polarization [8]. Moreover, strains of the WZ InGaN/GaN heterostructures, due to large lattice mismatch (11%) between InGaN and GaN [9], can induce a remarkable piezoelectric polarization [8,10]. This leads to a strong built-in electric field in the order of MV/cm in the heterostructures [3–6,11,12]. The electronic, dielectric and optical properties of the heterostructures are strongly affected by the built-in electric field. Thus, the performance of quantum devices based on WZ InGaN strained QDs can be affected by two important factors: the 3D confinement of the carriers in the QDs-like regions and the strong built-in electric field effect.

Exciton states and optical properties of WZ InGaN strained QDs have been investigated by experimental [3–6] and theoretical work [11,12]. However, few papers are involved in experimental and theoretical studies on impurity states in WZ InGaN strained QDs to date. More recently, Shi and Tansley [13] calculated the donor bound exciton binding energy in WZ InGaN strained QDs by means of a variational procedure. A deep understanding of the effects of impurities on electronic states of semiconductor nanostructures is a fundamental question in semiconductor physics because their presence can dramatically alter the performance of quantum devices [14]. In the past many years, there has much theoretical work on the binding energy of hydrogenic impurities in spherical quantum dot (QD) [15–18], cubic QD [19] and cylindrical QD [20]. Recently, Mendoza et al. [21] investigated stark effect dependence on hydrogenic impurity position in a cubic GaAs quantum box. Movilla and Planelles [22] dealt with dielectric mismatch effects on impurity binding energies in spherical QD. These studies show that the binding energy of hydrogenic donor impurities

* Corresponding author.
E-mail address: xiacongxin@sohu.com (C.X. Xia).

0375-9601/$ – see front matter © 2006 Elsevier B.V. All rights reserved.
doi:10.1016/j.physleta.2006.06.019

in nanoscopic systems depends upon materials and geometry (size and shape) and impurity position. However, none of these calculations included electric fields larger than 300 kV/cm. Nitride-based quantum heterostructures are subject to strong built-in electric field (MV/cm), which is different from the case of biased quantum wells (QWs) [11,12]. In this Letter, we will study variationally the binding energy of a hydrogenic donor impurity as functions of the impurity position and WZ InGaN strained QD structural parameters.

2. Theoretical model

According to previous theoretical studies on WZ InGaN strained QD [11,13], we consider an isolated cylindrical WZ $In_xGa_{1-x}N$/GaN strained QD with radius R and height L, surrounded by two large energy gap materials $In_yGa_{1-y}N$ ($y < x$) in the radial direction and GaN barrier layers along the growth axis z-direction, in which the origin is taken at the center of the QD and the z axis is defined to be the growth direction (see Fig. 1).

Within the framework of effective-mass approximation, the Hamiltonian for a hydrogenic donor impurity in the cylindrical WZ InGaN strained QD may be written as,

$$\hat{H} = \hat{H}_0 - \frac{e^2}{4\pi\varepsilon_0\bar{\varepsilon}r}, \tag{1}$$

with

$$\hat{H}_0 = -\frac{\hbar^2}{2m_{\parallel}^*}\left[\frac{1}{\rho}\frac{\partial}{\partial\rho}\left(\rho\frac{\partial}{\partial\rho}\right) + \frac{1}{\rho^2}\frac{\partial^2}{\partial\varphi^2}\right] - \frac{\hbar^2}{2m_{\perp}^*}\frac{\partial^2}{\partial z^2} + V(z) + V(\rho) - eFz, \tag{2}$$

where $r = \sqrt{(x-x_i)^2 + (y-y_i)^2 + (z-z_i)^2}$ is the distance between the electron and the impurity site, $x(x_i)$, $y(y_i)$ and $z(z_i)$ are the coordinates of the electron (impurity) in the QD, e is the absolute value of the electron charge, ε_0 is the permittivity of free space, and $\bar{\varepsilon}$ is the effective mean relative dielectric constant of the embedding material, $m_{\parallel}^*$ ($m_{\perp}^*$) is the electron in-plane (z-direction) effective mass, $V(z)$ and $V(\rho)$ are in-plane and the z-direction confinement potential due to the conductor band offset (Q) in the WZ InGaN/GaN strained QD, respectively, can be given by,

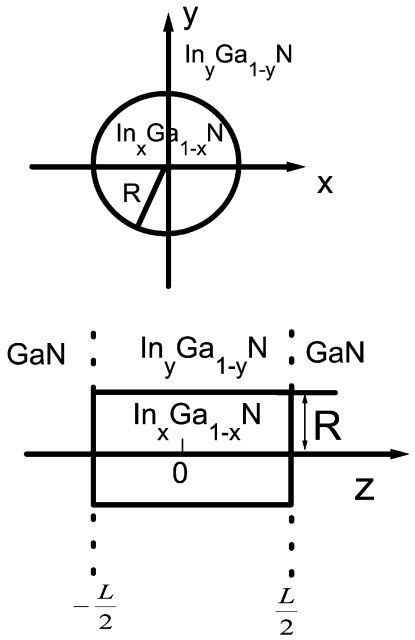

Fig. 1. A diagram of a cylindrical GaN/$In_xGa_{1-x}N$/GaN strained QD with radius R and height L, surrounded by two large energy gap materials $In_yGa_{1-y}N$ ($y < x$) in the radial direction and GaN in the z-direction.

$$V(\rho) = \begin{cases} 0, & \rho \leqslant R, \\ Q[E_g(In_yGa_{1-y}N) - E_g(In_xGa_{1-x}N)], & \rho > R, \end{cases} \tag{3}$$

$$V(z) = \begin{cases} 0, & |z| \leqslant \frac{L}{2}, \\ Q[E_g(GaN) - E_g(In_xGa_{1-x}N)], & |z| > \frac{L}{2}, \end{cases} \tag{4}$$

where $E_g(In_xGa_{1-x}N)$, $E_g(In_yGa_{1-y}N)$ and $E_g(GaN)$ are the band gap energies of the materials $In_xGa_{1-x}N$, $In_yGa_{1-y}N$ and GaN, respectively.

The strength of the built-in electric field F caused by the spontaneous and piezoelectric polarizations in the WZ InGaN/GaN strained QD is expressed as [11]

$$F = \begin{cases} \left|-\frac{P_{SP}^{InGaN} + P_{PE}^{InGaN} - P_{SP}^{GaN}}{\varepsilon_e^{InGaN}\varepsilon_0}\right|, & |z| \leqslant \frac{L}{2}, \\ 0, & |z| > \frac{L}{2}. \end{cases} \tag{5}$$

Here P_{SP}^{InGaN}, P_{PE}^{InGaN} and P_{SP}^{GaN} are the spontaneous and piezoelectric polarizations of InGaN and the spontaneous polarization of GaN, respectively. ε_e^{InGaN} is the electronic dielectric constant of material InGaN. In general, the direction of the built-in electric field F depends on the orientation of the spontaneous and piezoelectric polarizations and can be determined by both the polarity of the crystal and the strain of the quantum well (QW) structure. For Ga-faced GaN/InGaN/GaN QW, the built-in electric field F in the InGaN layer is pointed to the sample surface [8,11].

In order to calculate the ground-state energy of a hydrogenic donor impurity in the WZ InGaN/GaN strained QD, the trial wave function may be written as,

$$\Phi = \psi(\rho,\varphi,z)e^{-\alpha\rho_{ei}^2 - \beta z_{ei}^2}, \tag{6}$$

where $\psi(\rho,\varphi,z)$ is the eigenfunction of the Hamiltonian described in Eq. (2). The exponential term in Eq. (6) accounts for the presence of the hydrogenic impurity, α and β are variational parameters. $\rho_{ei}^2 = (x-x_i)^2 + (y-y_i)^2$ and $z_{ei}^2 = (z-z_i)^2$. We would like to point out that the two-parameter variational wave function is a reasonable choice for studying the WZ InGaN/GaN strained QD [11].

If we assume that the in-plane and on-axis motions of the electron are weakly coupled, as has been done in an isolated cylindrical WZ InGaN/GaN strained QD, the wave function $\psi(\rho,\varphi,z)$ can be written as [11]

$$\psi(\rho,\varphi,z) = f(\rho)h(z)e^{im\varphi}, \quad m = 0, \pm1, \pm2, \ldots, \tag{7}$$

where wave functions $f(\rho)$ and $h(z)$ describe the motions of the electron in plane and z-direction in the QD, respectively. m is the electron z-component angular momentum quantum number.

In this work, we are interested in the calculation of the ground-state of a hydrogenic donor impurity in the QD. Thus the trial wave function can be written as,

$$\Phi = f(\rho)h(z)e^{-\alpha\rho_{ei}^2-\beta z_{ei}^2}, \tag{8}$$

where the ground-state radial wave function $f(\rho)$ can be obtained using the 0-order Bessel function J_0 and the modified Bessel function K_0. For the z-axis motion of the electron, the wave function $h(z)$ can be expressed by the Airy functions Ai and Bi. If we ignore the existence of the built-in electric field, the z-axis wave function $h(z)$ can be obtained using linear combinations of analytical functions $\sin(\xi)$ and $\cos(\xi)$ (dot), or $\exp(\xi)$ (barriers).

The ground-state energy of a hydrogenic donor impurity in the WZ InGaN/GaN strained QD may be obtained by minimizing

$$E = \min_{\alpha,\beta} \frac{\langle\Phi|\hat{H}|\Phi\rangle}{\langle\Phi|\Phi\rangle}. \tag{9}$$

The ground-state donor binding energy E_b can be represented as follows,

$$E_b = E_0 - E, \tag{10}$$

where E_0 is the ground-state energy for the Hamiltonian of Eq. (2).

In order to investigate the influence of the QD confinement potential on the electron-impurity spatial separation, we define the in-plane and the growth axis z-direction mean quadratic distances $\bar{\rho}_{ei}$ and $\bar{z}_{ei}$,

$$\bar{\rho}_{ei} = \left(\frac{\langle\Phi|\rho_{ei}^2|\Phi\rangle}{\langle\Phi|\Phi\rangle}\right)^{\frac{1}{2}}, \tag{11}$$

$$\bar{z}_{ei} = \left(\frac{\langle\Phi|z_{ei}^2|\Phi\rangle}{\langle\Phi|\Phi\rangle}\right)^{\frac{1}{2}}. \tag{12}$$

3. Numerical results and discussion

We have calculated the ground-state donor binding energy E_b as functions of the impurity position z_i and the QD structural parameters, such as dot height L and radius R. Moreover, the effect of the strong built-in electric field due to spontaneous and piezoelectric polarizations is included. All material parameters used in the present article are the same as in Ref. [11].

In Fig. 2, the ground-state donor binding energy E_b is investigated as a function of the impurity position z_i. Fig. 2 shows that the donor binding energy E_b has a maximum value when the impurity position $z_i = 0$ if the built-in electric field is ignored. This is because the electron probability distribution is symmetric around $z_i = 0$. However, we can notice from Fig. 2 that the symmetry is broken and the maximum of the donor binding energy is shifted to the right side of the QD in the presence of the built-in electric field. The reason is that the built-in electric field moves the electronic probability density to the right side of the QD.

In Fig. 3, we show that the ground-state donor binding energy E_b as a function of the height L of WZ $In_{0.3}Ga_{0.7}N/GaN$ strained QD for different impurity positions z_i with (without) the built-in electric field. Fig. 3(a) shows that the donor binding energy curves A and E (B and D) are identical. It is also seen that the donor binding energy E_b for $z_i = 0$ (curve C) is larger than that for $z_i = \pm\frac{L}{2}$ (curve A or E) and $\pm\frac{L}{4}$ (curve B

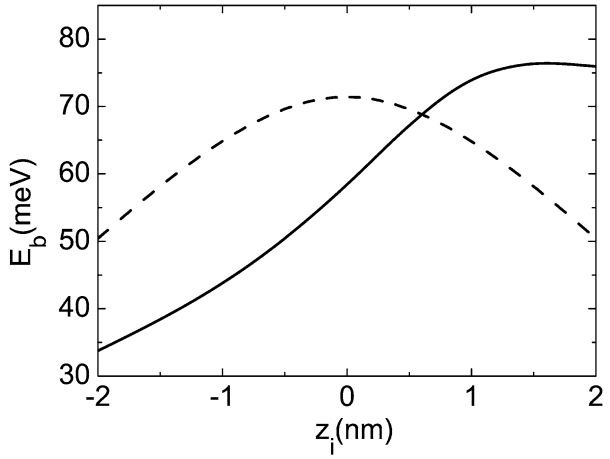

Fig. 2. The ground-state donor binding energy E_b as a function of the impurity position z_i for the $In_{0.3}Ga_{0.7}N/GaN$ QD with radius $R = 5$ nm and height $L = 4$ nm, surrounded by $In_{0.02}Ga_{0.98}N$ material in the radial direction. The solid (dashed) line is with (without) the built-in electric field.

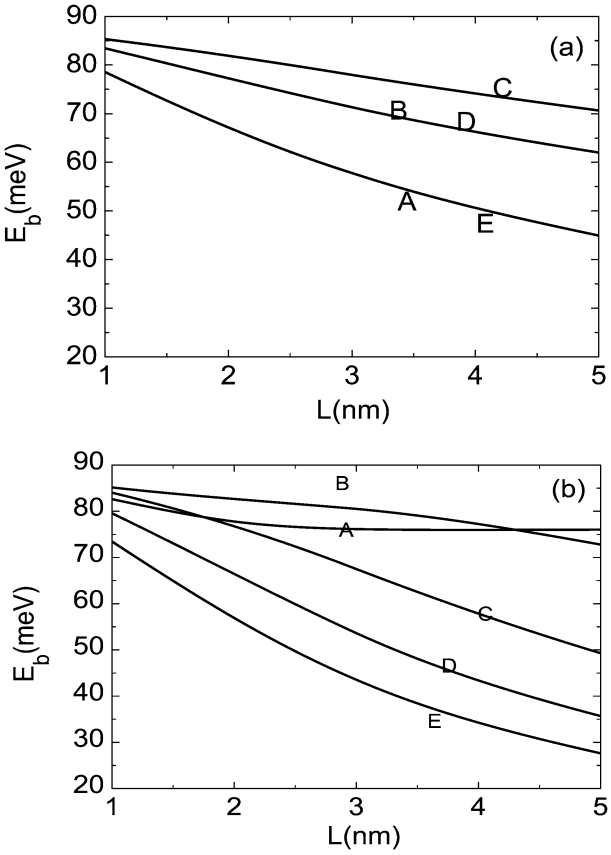

Fig. 3. The ground-state donor binding energy E_b as a function of the height L of the $In_{0.3}Ga_{0.7}N/GaN$ QD with radius $R = 5$ nm, surrounded by $In_{0.02}Ga_{0.98}N$ material in the radial direction, where the built-in electric field is ignored in (a) and considered in (b). The curves A, B, C, D and E are for the impurity positions $z_i = \frac{L}{2}, \frac{L}{4}, 0, -\frac{L}{4}$ and $-\frac{L}{2}$ nm, respectively.

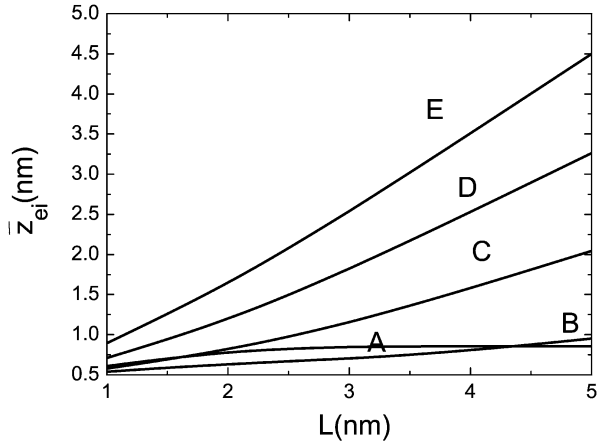

Fig. 4. Considering the effect of the built-in electric field, the distance $\bar{z}_{ei}$ between the electron and the impurity position z_i versus the height L of the $In_{0.3}Ga_{0.7}N/GaN$ QD with radius $R = 5$ nm, surrounded by $In_{0.02}Ga_{0.98}N$ material in the radial direction. The curves A, B, C, D and E have the same meaning as in Fig. 3, respectively.

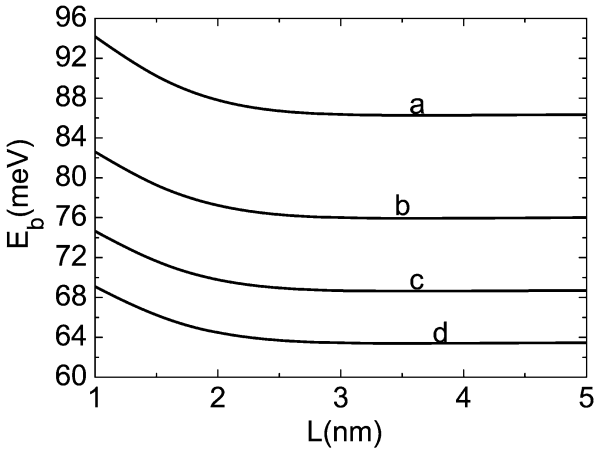

Fig. 5. The ground-state donor binding energy E_b versus the height L of the $In_{0.3}Ga_{0.7}N/GaN$ QD with the impurity located at $z_i = \frac{L}{2}$ for different values of the radius R, surrounded by $In_{0.02}Ga_{0.98}N$ material in the radial direction. The curves a, b, c and d are for the radius $R = 4, 5, 6, 7$ nm, respectively.

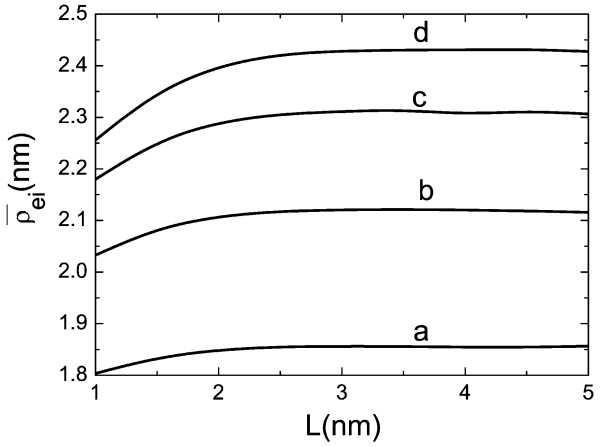

Fig. 6. Considering the effect of the built-in electric field, the distance $\bar{\rho}_{ei}$ between the electron and the impurity located at $z_i = \frac{L}{2}$ versus the height L of the $In_{0.3}Ga_{0.7}N/GaN$ QD for different values of the radius R, surrounded by $In_{0.02}Ga_{0.98}N$ material in the radial direction. The curves a, b, c and d have the same meaning as in Fig. 5, respectively.

or D). The reason is that the electron probability distribution is symmetric around $z_i = 0$ when the built-in electric field is ignored. Fig. 3(a) also shows that the E_b is decreased when L is increased in all cases. This is because the distance $\bar{z}_{ei}$ between the electron and the impurity is increased when L is increased.

However, we can see from Fig. 3(b) that the E_b along curves A and E (B and D) are split by the built-in electric field. Compared with Fig. 3(a), we can see that the built-in electric field induces only small difference of the E_b when dot height L is small. The splitting increases when the dot height L increases. This can be understood as follows. The symmetry of the electron probability distribution around $z_i = 0$ is broken due to the effect of the built-in electric field. For small dot height, the distance $\bar{z}_{ei}$ between the electron and the impurity has a small difference. The difference between the distances $\bar{z}_{ei}$ for $z_i = \pm\frac{L}{2}$ is increased when L is increased (see curves A and E in Fig. 4). The same applies for curves B and D in Fig. 4. Fig. 3(b) also shows that the donor binding energy E_b is decreased monotonically when the dot height L is increased for curves B, C, D and E, respectively. This is because the distance $\bar{z}_{ei}$ between the electron and the impurity is increased monotonically (see curves B, C, D and E in Fig. 4), the Coulomb interaction is reduced and the donor binding energy decreases. In particular, Fig. 3(b) shows that the E_b of the impurity located at $z_i = \frac{L}{2}$ tends towards a constant value when dot height $L \geqslant 2.5$ nm (curve A). The reason for such a behavior as follows. The strong built-in electric field pushes the electron towards the right side of the QD, the distance $\bar{z}_{ei}$ between the electron and the impurity remains insensitive to the dot height (see curve A in Fig. 4).

Considering the built-in electric field effect, we further investigate the ground-state donor binding energy E_b versus the height L of the WZ $In_{0.3}Ga_{0.7}N/GaN$ strained QD with the impurity located at $z_i = \frac{L}{2}$ in Fig. 5 for different values of the dot radius R. We can observe from Fig. 5 that the behavior of the donor binding energy E_b is quite similar, and the E_b is independent of the dot height when dot height $L \geqslant 2.5$ nm in all cases. This can be understood as follows. When dot height L ($\geqslant 2.5$ nm) is increased, the distance $\bar{\rho}_{ei}$ between the electron and the impurity located at $z_i = \frac{L}{2}$ is independent of the dot height L in all cases (see Fig. 6). This result could be of interest for technological purpose, as it could involve a source of control some impurity-related properties in these systems. Fig. 5 also shows that the donor binding energy E_b decreases if R increases. The reason is that the distance $\bar{\rho}_{ei}$ is increased (see Fig. 6), the Coulomb interaction is decreased when R is increased.

4. Conclusions

In conclusion, we have variationally calculated the ground-state binding energy of a hydrogenic donor impurity located anywhere along the growth axis in the WZ InGaN/GaN strained QD, within the framework of effective-mass approximation. Numerical results show that the donor binding energy is highly dependent on the impurity position, and the strong built-in elec-

tric field induce an asymmetrical distribution of the donor binding energy versus the center of the QD. In particular, we found that the donor binding energy is independent of the dot height when the impurity is located at the right boundary ($z_i = \frac{L}{2}$) of the $In_{0.3}Ga_{0.7}N/GaN$ strained QD with dot height $L \geqslant 2.5$ nm. The physical reasons have been analyzed in-depth. Experimental results for hydrogenic donor impurity in WZ InGaN/GaN strained QD are still lacking at present. We hope that our calculation results can stimulate further investigations of the physics, as well as device applications of group-III nitrides.

Acknowledgements

This work was supported by the National Natural Science Foundation of China under Grant No. 60476047, by the Natural Science Foundation of the Education Bureau of Henan Province, China under Grant No. 2004140004 and the Natural Science Foundation of Henan Province, China under Grant No. 0611053800.

References

[1] B. Gil, Group III Nitride Semiconductor Compounds, Clarendon Press, Oxford, 1998.
[2] S. Nakamura, S.F. Chichibu, Introduction to Nitride Semiconductor Blue Lasers and Light Emitting Diodes, Taylor and Francis, London, 2000.
[3] R.A. Taylora, J.W. Robinsona, J.H. Ricea, A. Jarjoura, J.D. Smitha, R.A. Oliverb, G.A.D. Briggsb, M.J. Kappersc, C.J. Humphreysc, Y. Arakawad, Physica E 21 (2004) 285.
[4] V.P. Solorzano, M. Ubl, H. Grabeldinger, A. Groning, H. Schweizer, M. Jetter, Physica E 26 (2005) 133.
[5] J. Kim, K. Samiee, J.O. White, J.M. Myoung, K. Kim, Appl. Phys. Lett. 80 (2002) 989.
[6] P. Ruterana, S. Kret, A. Vivet, G. Maciejewski, P. Dluzewski, J. Appl. Phys. 91 (2002) 8979.
[7] Y. Masumoto, T. Takagahara, Semiconductor Quantum Dots, Springer, Berlin, 2002.
[8] O. Ambacher, J. Phys. D 31 (1998) 2653.
[9] P. Waltereit, M.D. Craven, S.P. DenBaars, J.S. Speck, J. Appl. Phys. 92 (2002) 456.
[10] F. Bernardini, V. Fiorentini, D. Vanderbilt, Phys. Rev. Lett. 79 (1997) 3958.
[11] J.J. Shi, Z.Z. Gan, J. Appl. Phys. 94 (2003) 407.
[12] C.X. Xia, S.Y. Wei, Phys. Lett. A 346 (2005) 227.
[13] J.J. Shi, T.L. Tansley, Solid State Commun. 138 (2006) 26.
[14] T. Ando, Y. Arakawa, K. Foruka, S. Komiyama, H. Nakashima, Mesoscopic Physics and Electronics, Springer, Berlin, 1998;
H.J. Queisser, E.E. Haller, Science 281 (1998) 945.
[15] J.L. Zhu, X. Chen, Phys. Rev. B 50 (1994) 4497.
[16] D.S. Chuu, C.M. Hsiao, W.N. Mei, Phys. Rev. B 46 (1992) 3898.
[17] N.P. Montenegro, S.T.P. Merchancano, Phys. Rev. B 46 (1992) 9780.
[18] C. Bose, J. Appl. Phys. 83 (1998) 3089.
[19] C.I. Mendoza, G.J. Vzquez, M.D.C. Mussot, H.N. Spector, Phys. Status Solidi C 1 (2004) S74.
[20] F.J. Ribeiro, A. Latge, M. Pacheco, Z. Barticevic, J. Appl. Phys. 82 (1997) 270.
[21] C.I. Mendoza, G.J. Vazquez, M.D.C. Mussot, H. Spector, Phys. Rev. B 71 (2005) 075330.
[22] J.L. Movilla, J. Planelles, Phys. Rev. B 71 (2005) 075319.